Towards complete band structure of microscopic MoS_2 flakes.

Sergey Babenkov[1], Marie Froidevaux[2], Peng Ye[1], Ludovic Tortech[1], Yannick Dappe[1], Willem Boutu[1], Nickolas Barrett[1], and Hamed Merdji[2]

1 Université Paris-Saclay, CEA, CNRS, 91191 Gif-sur-Yvette, France
2 LOA, ENSTA Paris, CNRS, Ecole Polytechnique, 91762 Palaiseau, France

Abstract. The occupied and unoccupied electronic states of MoS_2 monolayer isolated flake were studied using laboratory based photoemission electron microscope (PEEM) nanoESCA equipped with He-I photon source. PEEM real-space imaging allowed selecting the high quality flake. Altogether, the data will allow accurately recovering the band structures of MoS_2. The band structures will be used in future pump-probe experiments to explore the dynamics of electrons in the conduction band and photo-induced multi-topological states using trefoil polarization.

Introduction

Since the discovery of graphene in 2004, the interest of solid-state physics and the material science community in graphene-like two-dimensional (2D) materials has exploded. During the past decade, various methods have been developed to synthesize and manipulate them. Transition-metal dichalcogenides (TMDC) (MX_2 layers with 2H symmetry where M = Mo, W; X = S, Se, Te) occupy a special place in the class of 2D-materials thanks to their fascinating properties [1, 2, 3]: direct band gaps at monolayer thickness, both chemically inert and stable surfaces at room temperature and topological states.

Recently, it has been theoretically shown that a topological phase transition can be stimulated entirely with shaped light fields, such as trefoil polarization states, in conventional hexagonal materials [4]. The idea is based on nonlinear interaction of monolayer MoS_2 and the bicircular field (trefoil polarization). Such light fields with trefoil symmetry [5] and complex orbital angular momenta [6] have already been generated using higher laser harmonics. Trefoil polarization can be created combining ω and 2ω photons with circular polarization of opposite helicity. In the experiment, the orientation of the trefoil with respect to MoS_2 structure can be controlled either by phase delay φ between two pulses or by sample rotation. For example, when $\varphi = -\pi/2$, both sublattices are addressed equally. As a result, the K and K' valleys are nearly equally excited. When $\varphi = 0$, the cycle-averaged band structure shows a strong valley asymmetry. This reflects in the valley populations, which show strong contrast. The situation is reversed for $\varphi = \pi$, where the electron population switches to the opposite valley. The overall helicity of the field also contributes to the valley asymmetry, but its effect is relatively weak. It manifests in small valley polarization for $\varphi = \pm\pi/2$, and in that $\varphi = 0$ and $\varphi = \pi$ are not exact opposites.

This opens a route towards a new device based on electronic topology and ultrashort light pulses. In particular, by orienting the trefoil symmetry it is possible to populate alternatively K and K' valleys in the conduction band and measure their dynamics using pump-probe experiments. This is one of the goals of our H2020 project "OPTOlogic" [7].

The first question is therefore to measure the band structure at the surface of a single flake. The possibility to obtain the information about unoccupied states was predicted [8,9] and recently explored using laboratory based equipment [10]. In practice, the k-space intensity maps taken in the energy range of secondary electrons, secondary electron emission microscopy (k-SEEM), will consist of the local intensity minima and maxima, which indicate the unoccupied bands. The available energy range depends on the electron effinity of the given sample. The lower electron affinity is, the more closer vacuum level is to conduction band minimum (or even vacuum level lies below conduction band minimum), the large is available energy region in *k*-SEEM.

With this idea in mind, in this work we studied the occupied and unoccupied states of isolated MoS_2 monolayer flakes on top of SiO_2/Si wafer by means of XPS, k-PEEM and k-SEEM.

Experimental details

In this study, we were using commercially available CVD-grown monolayer 2H-MoS2 flakes purchased from 6carbon technology [11]. The flakes are grown on top of a 300nm-SiO2/Si wafer (source substrate) which makes the photoemission experiments impossible due to the charging of the SiO_2 surface. One way to overcome this problem is to transfer the flakes from source substrate to Si wafer with thin (2-3 nm) SiO_2 layer (target substrate). It has 2 advantages: (i) the layer of the

SiO_2 is thick enough to supress the band features of the Si crystal allowing the photoemission experiment and (ii) thin enough to avoid possible charging effects using X-ray photoemission spectroscopy (XPS), Figure 1. XPS spectra were recorded at 3 different emission angles: normal (90°), intermediate (55°), grazing (20°). No detectable shifts due to charging of the surface was observed, while the thickness of the SiO_2 was estimated to be 2-3 nm.

In order to transfer flakes from source to target substrate, we used surface energy-assisted transfer which is described in detail elsewhere [12]. In short, the source wafer was covered by the thin membrane of Polystyrene using polystyrene/toluene solution and spin-coating (3500RPM , 60´´). Later the polystyrene membrane is dried on the hot plate (80°C, ~15´). Using deionized water we detached the membrane and flakes from the wafer. The floating membrane was caught by a target wafer. The residual water between membrane and wafer surface was removed by a paper towel following by gentle heating on the hot plate (40°C, ~20´). The polystyrene membrane was dissolved in toluene bathes in 3 steps (~ 20´ each). Finally, the wafer was splashed with ethanol and dried by purified nitrogen.

The residual contamination was desorbed by annealing at 450°C during 30 min in nanoESCA preparation chamber. It allowed considerably improve the quality of the k-PEEM images. The sample was *in-situ* moved to the analytical chamber for PEEM measurements.

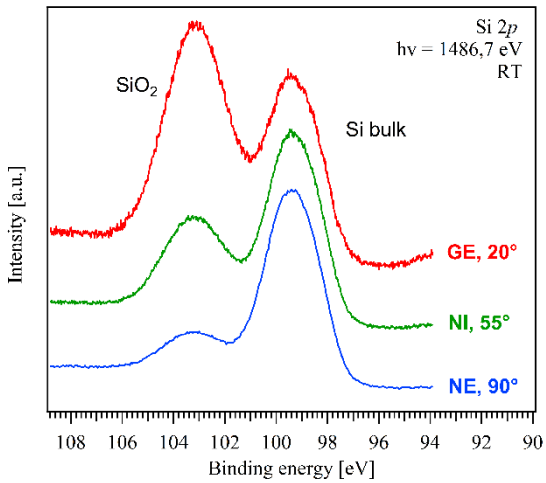

Figure 1. XPS Si 2p spectra taken at different electron emission angles from normal (90°) to grazing (~20°).

The nanoESCA analytical chamber is equipped with Hg (~ 4.9 eV) and He-I (21.2 eV) photon sources allowing best real-space and k-space resolution. The sample manipulator in nanoESCA analytical chamber allowing reproducible precise manipulation with sample and bring the region of interest to field of view even after transfers of sample to the preparation chamber and back to analytical chamber. Therefore, it is possible to study exactly the same MoS_2 flake after sample annealing and/or deposition of thin films.

Results and discussion

Figure 2 presents large field of view (a) and detailed (b) real-space images of the MoS_2 flakes taken using Hg (hv~ 4.9 eV) photon source. It is clear that the flakes are distributed randomly in terms of size, shape and orientation over the sample surface. Therefore, in order to select single isolated flake of best quality for k-PEEM measurements the real-space microscopic capabilities of nanoESCA are essential. The region selected for k-PEEM measurements is highlighted on figure 2 (b) by yellow lines.

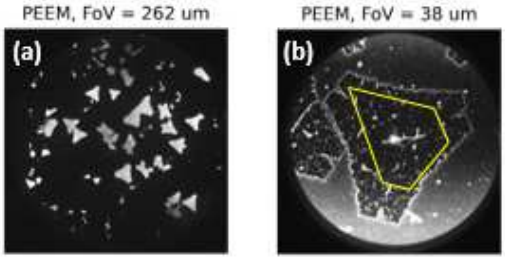

Figure 2 Large field of view (a) and detailed (b) real space PEEM images taken using Hg photon source (~4.9eV). The region of the flake selected by iris for k-PEEM is highlighted by yellow lines.

Thanks to the thin SiO_2 chemical oxide, there are no detectable image and spectra distortions caused by charging under photoemission. Consequently, the polystyrene-based chemical transfer allows creating $MoS_2/SiO_2/Si$ sample of sufficiently good quality for photoemission experiments avoiding intermediate conduction buffer layer, as was proposed by S.W. Jung et al. [13].

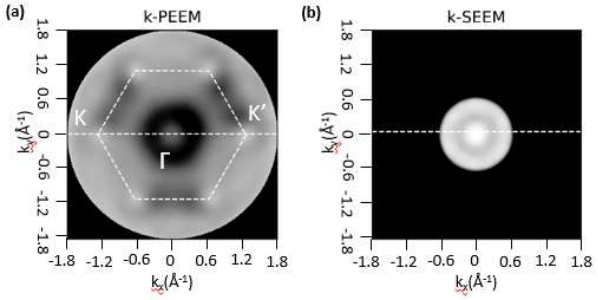

Figure 3 *2nd derivative of constant energy cuts I(E; kx, ky) taken on single MoS2 flake: (a) valence band structure taken at 1.4 eV binding energy and (b) the structure of unoccupied states in the second electron emission tail at 15.5 eV binding energy. The data were acquired using He-I emission (hv = 21.2 eV) at 30K sample temperature.*

Figure 3 presents the second derivative of *k*-photoemission electron microscopy (k-PEEM) momentum sections $I(E; k_x, k_y)$ in the regions close to Fermi level (a) and in the secondary electron tail (b) taken on a single MoS_2 flake. On panel (a) the valence band structure at 1.4 eV binding energy is presented. The high symmetry points K, K´ found themselves at the vertices of hexagon and Γ in the center of hexagon are highlighted. It is clear that the intensity of the signal in panel (b) is strongly modulated.

Fig. 4 presents the E-*k* cuts through K-K´direction of the data stacks along the straight dashed lines in Figure 3(a)

for k-PEEM region and Figure 3 (b) for k-SEEM region. Black dashed lines in figure 4 indicate on the slice where the data for figure 3 were taken. In case of k-SEEM the accessible region of the energy and $k_{\parallel}$ is limited by electron affinity and free-electron dispersion parabola defined by the relation $E = \frac{\hbar^2 k_{||}^2}{2m_e}$. It is highlighted by yellow dashed line. One way to get information about the unoccupied states closer to the conduction band minimum is to lower the effective work function (WF) of the sample, for example by deposition of Cs thin film. The expected available region is highlighted by blue dashed line. The figure 4 presents the calculated occupied and unoccupied states. First-principles calculations have been performed using a DFT localized orbital molecular dynamic technique (FIREBALL) [14-17]. In this study, we have considered a standard (1 x 1) unit cell of MoS_2. A set of 300 special k points along the G-K-M path has been used for the band structure calculations.

In case of occupied states, the k-PEEM data are in good agreement with theory. However, there is a clear difference in theory and experimental data on unoccupied states. One of the possible reasons is that the available kinetic energy range given by the He I photon beam is too short (~17eV). The occupied and unoccupied states could overlap. In order to expand the kinetic energy range and separate the states it is necessary to use a photon beam of higher energy, for example at the synchrotron (hv~100-200eV). In this case, the secondary emission tail will appear at much higher kinetic energies that allows large kinetic energy gap between the occupied states near fermi level and unoccupied states in secondary emission tail.

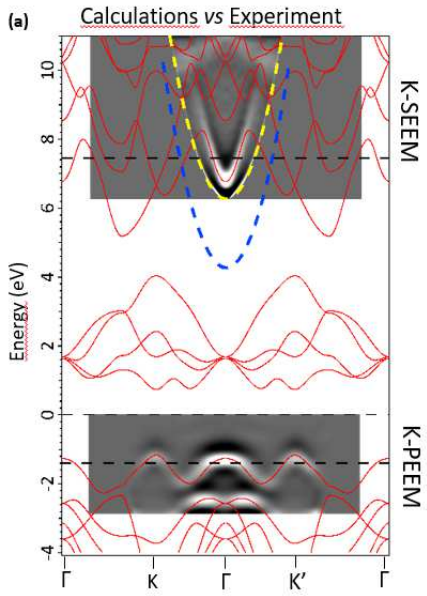

Figure 4. Calculated occupied and unoccupied electronic states and corresponding experimental k-PEEM. E-k cuts through K-Γ-K' as shown by horizontal, white dashed lines in Figure 3 (a, b).

Conclusions

The presented results shows that the band structure of MoS_2 isolated monolayer flakes on 2-3nm SiO_2/Si wafer can be studied by means of photoemission experiment. No harmful surface charging effects were detected. The possibility to study the unoccupied states was limited by the available kinetic energy range provided by He I emission. This could be overcome by using photons of sufficiently higher energy, for example using synchrotron radiation. In addition, it is possible to lower work function by deposition of Cs thin film on the surface of the sample.

Acknowledgements

We want to acknowledge Dr. Vincent Derycke and Nathan Ullberg (CEA-Saclay, IRAMIS) for help with sample preparation and fruitful discussion of the results. We want to acknowledge support from OPTOlogic European project Nr EUR830OPTOLO.

References

1. C. Jin, E.Y. Ma, O. Karni, E.C. Regan, F. Wang and T.F. Heinz., Nature Nanotechnology **13**, 994–1003 (2018)

2. M. Chhowalla, H.S. Shin, G. Eda, L.-J. Li, K. P. Loh and H. Zhang, Nature Chemistry **5**, 263–275 (2013)

3. B.A. Bernevig, T.L. Hughesand, and S.-C. Zhang, Science **314**, 1757 (2006)

4. R.E.F. Silva, Á. Jiménez-Galán, B. Amorim, O. Smirnova and M. Ivanov, Nature Photonics **13**, 849–854 (2019)

5. A. Fleischer, O. Kfir, T. Diskin, P. Sidorenko and O. Cohen, Nature Photon **8,** 543–549 (2014)

6. L. Rego, K.M. Dorney, N.J. Brooks, Q.L. Nguyen, C.-T. Liao, J.S. Román, D.E. Couch, A. Liu, E. Pisanty, M. Lewenstein, L. Plaja, H.C. Kapteyn, M.M. Murnane, and C. Hernández-García., Science **364** (6447), 1253 (2019)

7. https://cordis.europa.eu/project/id/899794

8. R. Feder and J. B. Pendry, Solid State Commun. 26, 519 (1978)

9. M. Bovet, V. N. Strocov, F. Clerc, C. Koitzsch, D. Naumović, and P. Aebi 1, Phys. Rev. Lett. 93, 107601 (2004)

10. G. Wan, A. Croot, N.A. Fox, M.Cattelan, Adv. Funct. Mater. **2021**, 31, 2007319

11. http://www.6carbon.com/index-en.php

12. A. Gurarslan, Y. Yu, L. Su, Y. Yu, F. Suarez, S. Yao, Y. Zhu, M. Ozturk, Y. Zhang, and L. Cao, ACS Nano 2014, 8, 11, 11522–11528

13. S.W. Jung, S. Pak, S. Lee, S. Reimers, S. Mukherjee, P. Dudin, T.K. Kim, M. Cattelan, N. Fox, S.S. Dhesi, C. Cacho, and S.N. Cha, Applied Surface Science **532** (2020) 147390

14. J. Lewis, et al., Phys. Rev. B 64 (2001) 195103.

15. J.P. Lewis, et al., Phys. Status Solidi 248 (2011) 1989-2007.

16. P. Jelínek, H. Wang, J. Lewis, O. Sankey, J. Ortega, Phys. Rev. B 71 (2005) 235101.

17. O.F. Sankey, D.J. Niklewski, Phys. Rev. B 40 (1989) 3979-3995.